Title

Neurexin Family Member Contactin-Associated Protein Like-4 (CNTNAP4) is a specific cell membrane receptor of Neural EGFL Like 1 (NELL1)

Author

Chen, Eric

Publication Date

2018

Peer reviewed|Thesis/dissertation

UNIVERSITY OF CALIFORNIA

Los Angeles

Neurexin Family Member Contactin-Associated Protein Like-4 (CNTNAP4) is a specific cell membrane receptor of Neural EGFL Like 1 (NELL1)

A thesis submitted in partial satisfaction

of the requirements for the degree Master of Science

in Oral Biology

by

Eric C Chen

2018

ABSTRACT OF THE THESIS

Neurexin Family Member Contactin-Associated Protein Like-4 (CNTNAP4) is a specific cell membrane receptor of Neural EGFL Like 1 (NELL1)

by

Eric C Chen

Master of Science in Oral Biology

University of California, Los Angeles, 2018

Professor Kang Ting, Chair

Secretory protein neural EGFL like 1 (Nell-1) has been shown to exert potent osteogenic effects in multiple small and large animal models. Here, we identified and validated contactin-associated protein-like 4 (Cntnap4) as the first Nell-1 specific cell surface receptor. Cntnap4, a transmembrane neurexin superfamily protein member, has critical functions in neurodevelopment but no known function in osteogenesis. In the present study, we demonstrate that: 1) Nell-1 and Cntnap4 co-localize on the surface of osteogenic-committed cells, 2) Nell-1 and Cntnap4 exhibit high-affinity interactions, 3) Cntnap4 knockdown reduces Nell-1-responsive osteogenesis, and 4) Cntnap4 mediates Nell-1-activated MAPK and Wnt signaling in osteogenic-committed cells. Taken together, these findings and recent literature further the notion of potential neuroskeletal interplay. This unanticipated discovery connecting Cntnap4 to Nell-1 during osteogenesis provides

a foundational framework for further exploration of a novel functional axis as it relates to skeletal and potential neuronal function.

The thesis of Eric C Chen is approved.

Tara Aghaloo

Jin Hee Kwak

Bo Yu

Kang Ting, Committee Chair

University of California, Los Angeles

2018

TABLE OF CONTENTS

Abstract……iii-iv

Introduction……..……..1-2

Materials and Methods

Nell-1 protein purification and Cntnap4 plasmid construction...……..3

Phage display biopanning and ELISA…….……..,……...4

Gene expression profiling and Immunocytochemistry staining……5

Histological analysis and the Duolink® proximity ligation assay…….6

RNA interference (RNAi) and In vitro osteogenic differentiation assays…….7

Statistical analysis……8

Results

T7 phage particles with 1st and 2nd Cntnap4 LamG extracellular domains exhibit high binding affinity to Nell-1……...9

Nell-1 and Cntnap4 bind on the plasma membrane of osteogenic-committed cells …...……....9

Cntnap4 knockdown reduces Nell-1-responsive osteogenesis……...10

Cntnap4 mediates Nell-1-activated MAPK and Wnt signaling in osteogenic-committed cells……11

Discussion……..……..12-15

Conclusion……..……..16

Figures and Tables……..……17-29

References……..……..30-35

LIST OF TABLES

Table 1: Cell lines and primary cells used for Cntnap4 expression screening……...17

Table 2: Primer and probe sets used for real-time PCR …….18

Table 3: Primary antibodies used for immunohistochemistry staining and Western blot analysis……...19

Table 4: Nell-1-binding candidate proteins screened by phage biopanning ……..20

LIST OF FIGURES

Figure 1: Schematic of phage biopanning.……..…..…….……..... ……..21

Figure 2: Binding affinity confirmation between Cntnap4 phages and Nell-1.....22

Figure 3: Cntnap4 mRNA expression levels in twelve types of non-neuron and glial cells…….24

Figure 4: Cntnap4 and Nell-1 co-localize on the surface of osteogenic-committed cells and in mouse calvarial bone …….25

Figure 5: Cntnap4 is essential for Nell-1 osteogenic bioactivity *in vitro* ……...……...26

Figure 6: Cntnap4 is essential for Nell-1-activated MAPK and Wnt signaling *in vitro*……28

Acknowledgments

This work was supported by the NIAMS (R01 AR066782-01, AR068835-01A1, AR061399-01A1), UCLA/NIH CTSI UL1TR000124, the National Aeronautics and Space Administration GA-2014-154, the International S&T Cooperation Program of China (No. 2013DFB30360), and the National Natural Science Foundation of China (No. 81200762).

This project would not have been possible without the assistance, advice, and support of a number of individuals. First and foremost, I would like to sincerely thank Drs. Chenshuang Li and Zhong Zheng for their expert advice and outstanding technical expertise in all aspects of this body of work from conception to completion. I would also like to thank Drs. Xiaoyan Chen, Wenlu Jiang, and Feng Cheng for their technical expertise and support. Finally, I would like to thank Drs. Kang Ting, Xinli Zhang, and Chia Soo for their mentorship, understanding, and guidance.

Introduction

Neural EGFL like 1 (Nell-1) is a unique multimeric secretory protein (1). Nell-1 was first sequenced by Watanabe *et al.* from a human fetal brain cDNA library (2). Ting *et al.* first identified the osteogenic function of Nell-1 from its high expression in active bone formation sites in human craniosynostosis patients, finding that *Nell-1* was preferentially expressed in cranial intramembranous bone and neural tissues (3). Over the years through various gain- and loss-of-function models, the critical role of Nell-1 in craniofacial and appendicular skeletogenesis has been thoroughly investigated (4-6). For instance, *Nell-1*-deficient newborn mice have been shown to have reduced calvarial bone growth, widened sagittal sutures, and short overall body lengths (1, 5, 7). Confirming the importance of Nell-1 in human development, a similar phenotype was recently reported in a 3-year-old Japanese girl with a *Nell-1* gene locus deletion where she demonstrated delayed cranial fontanelle and suture closure as well as a short body stature (8).

Notably, the osteogenic potential of Nell-1 has been validated in various small and large animal models including rodents, sheep, and non-human primates (9-13). In fact, Nell-1 may hold great potential as an alternative therapeutic option for local and systemic bone regeneration due to its excellent safety profile, tumor-suppressive properties, and significant benefits in preventing osteoporotic bone loss (11, 14-15) . This stands in stark comparison to bone morphogenetic protein 2 (BMP2), the current Food and Drug Administration (FDA) approved gold standard for bone graft substitutes. Specifically, BMP2 has a number of well-documented, off-target effects that have not been observed after Nell-1 administration such as post-operative inflammation, adipogenesis, osteoclastogenesis, adipogenesis, and ectopic bone formation (13, 16-19). While such off-target effects hinder the clinical applications of BMP2, the pharmacokinetics of Nell-1 have been further shown to improve with the FDA-approved method of PEGylation, where Nell-1 was covalently

conjugated with water-soluble polyethylene glycol (PEG) molecules (20-22). In doing so, PEGylation of NELL-1 was successfully shown to prolong its half-life and increase thermal stability without compromising osteogenic effects or resulting in notable cytotoxicity (23).

With regards to its structure, Nell-1 is a secretory extracellular protein that contains a secretory signal peptide, an N-terminal laminin G (LamG) domain which overlaps with a thrombospondin-1-like (TSPN) module, several von Willebrand factor-like repeats with five chordin-like, cysteine-rich (CR) domains, and six epidermal growth factor (EGF)-like repeats (1, 24). While Nell-1's combination of LamG domain, CR domains, and EGF-like repeats suggests that is possesses specific ligand-receptor interactions, Nell-1 has not been shown to interact with any known EGF-like receptors (3, 15, 25, 26).

On the other hand, contactin-associated protein-like 4 (Cntnap4, also known as Caspr4) is a transmembrane neurexin superfamily protein member with important functions in neurocognition, neurodevelopment, and neuronal cell communication (27-29). Cntnap4 belongs to a large category of synaptic cell adhesion molecules that have been implicated in a diverse number of neuropsychiatric and neurodevelopmental disorders (30). Located on the presynaptic membrane of interneurons, Cntnap4 regulates inhibitory interneuron synapse maturation and synaptic transmission in dopaminergic neurons and GABAergic neurons alike. In fact, murine *Cntnap4*-null mice demonstrate significant interneuron dysfunction and display perseverative behaviors that mimic common behavioral abnormalities seen in individuals with autism spectrum disorders (ASDs) (28). Since the initial account of Cntnap4 in 2002 (27), there have yet to be any known extracellular ligands found to be associated with this family of essential neuronal proteins. In the present study, a novel interaction between Nell-1 and Cntnap4 during osteogenesis was identified and verified for the first time.

Materials and Methods

Nell-1 protein purification

Recombinant full-length human Nell-1 with polyhistidine-tags (His–tagged Nell-1) was obtained from Katayama Inc. (Amagasaki-city, Hyogo, Japan), and used as bait in the phage display study. Recombinant full-length human Nell-1 without tags was obtained from Aragen Bioscience Inc. (Morgan Hill, CA, USA) with a purity of 92% (19) for all functional studies. The plasmid expressing LamG domain deleted human Nell-1 (Nell-$1_{[LamG]}$), constructed from the pcDNA^{TM}3.1/*myc*-His B Mammalian Expression Vector was transfected into CHO-K1 cells (ATCC® CCL-61^{TM}; ATCC, Manassas, VA, USA) by Lipofectamine® 3000 (32). The His-tagged Nell-$1_{[LamG]}$ was then purified from the supernatant of the transient transfection product using the ProBond^{TM} Purification System (Thermo Fisher Scientific, Canoga Park, CA, USA).

Cntnap4 plasmid construction and recombinant protein purification

The open reading frame sequence of human *Cntnap4* (NM_033401) was obtained from GenScript (Piscataway, NJ, USA). The extracellular portion of Cntnap4 (Cntnap4^{extra}) was subcloned into pSecTag2A Mammalian Expression Vector (Thermo Fisher Scientific) with the primers 5'-CAC GGT ACC TGG GAA TTC CTA T-3' and 5'-TTA CTC GAG CTG CAG AGT CAC TT-3', and then transfected into CHO-K1 cells. Next, the His-tagged Cntnap4^{extra} was purified from the supernatant of the transient transfection product using the ProBond^{TM} Purification System (Thermo Fisher Scientific) and identified by Western Blot analysis.

Phage display biopanning

HIS-Select® Nickel Magnetic Agarose Beads (Sigma-Aldrich Corp., St. Louis, MO, USA) were selected to immobilize His-tagged Nell-1. The phage display cDNA library was constructed from the Human Brain cDNA Library using the Novagen T7Select® System (EMD Millipore, Billerica, MA, USA). An aliquot of the amplified phage display cDNA library was incubated with His-tagged Nell-1 coated beads for four rounds of biopanning screens. Subsequently, the phages bound to the His-tagged Nell-1 coated beads were eluted, and 100 plaques were selected to amplify the phage DNA by PCR with the provided primers and buffers in the Novagen T7Select® System. Sequences spanning over 500 bp in size were selected and sequenced by Laragen Inc. (Culver City, CA, USA) (**Fig. 1**).

ELISA

Dissociation constant ELISA was performed per manufacturer instructions from Novagen T7 Tail-Fiber Monoclonal Antibody (EMD Millipore). In short, 10 μg/ml of His-tagged full-length Nell-1 or Nell-$1_{[LamG]}$ was used as bait to coat the ELISA plate (Corning Inc., New York, NY, USA). After removing the unbounded bait, the plate was blocked with 3% non-fat milk overnight at 4°C. 100 μl/well diluted phage lysate ($1X10^4$ – $1X10^{10}$ phages/ml) was added to the coated plate, and incubated at 37°C for 1 hour. Unbound phages were thoroughly washed out with 1X Tris-buffered saline with 0.1% Tween 20 (TBST) buffer. T7 Tail-Fiber Monoclonal Antibody (1:2000) was added for 1-hour incubation prior to the addition of HRP-conjugated anti-mouse secondary antibody (1:1000; Abcam, Cambridge, MA, USA). 1-Step™ Ultra TMB-ELISA Substrate Solution (Thermo Fisher Scientific) was utilized for developing. After acidification by 2M sulfuric acid (Sigma-Aldrich Corp.), absorbance of the reaction product was measured by an Epoch Microplate spectrophotometer (BioTek, Winooski, VT, USA) at 450 nm. Each concentration of

phage was tested in triplicate, while empty T7 phages (without a cDNA insert) were used as the negative controls.

Gene expression profiling

Based on previously published functional investigations of Nell-1, 12 different cell lines and primary cells isolated from bone or relevant tissues were selected for use in the current study (**Table 1**). Total RNA was isolated from subconfluent cells by TRIzol® Reagent, followed by DNase treatment. 1 μg RNA was injected for reverse transcription (RT) with the iScript™ Reverse Transcription Supermix for RT-qPCR (Bio-Rad Laboratories Inc., Hercules, CA, USA). 1 uL reverse transcription product was used for real-time PCR with SsoAdvanced™ Universals Probes Supermix (Bio-Rad Laboratories Inc.) and TaqMan® primers/probe sets (**Table 2**; Thermo Fisher Scientific) on a QuantStudio3 system (Thermo Fisher Scientific) in triplicate.

Immunocytochemistry staining

Serum-starved MC3T3-E1 pre-osteoblasts (Subclone 4, ATCC® CRL-2593™; ATCC, Manassas, VA, USA) and primary newborn mouse calvarial cells (6) were treated with 500 ng/ml Nell-1 for 30 min and fixed with ice-cold acetone. The fixed cells were blocked with 3% bovine serum albumin (BSA; Sigma-Aldrich Corp.) and incubated with primary antibodies (**Table 3**) in IHC-Tek™ Antibody Diluent (pH 7.4; IHC World, LLC, Woodstock, MD, USA) overnight at 4°C. Following three washes with 1x PBST, cells were incubated with FITC-conjugated anti-rabbit IgG and Texas Red-conjugated anti-Goat IgG secondary antibodies (Abcam), and counterstained with DAPI Fluorescence Stain (Cell Biolabs, Inc., San Diego, CA, USA). Co-localization of Nell-1 and Cntnap4 was documented by confocal laser scanning microscopy (CLSM) on a Leica TCS SP8

Confocal Laser Scanning Platform coupled with Leica Application Suite X software (Buffalo Grove, IL, USA).

Histological analysis and Immunohistochemical staining

C57BL/6 mice were bred and maintained under an institutionally approved protocol provided by the Chancellor's Animal Research Committee at UCLA as previously described (33). Calvarial tissues dissected from 60-day-old P60 mice were fixed in 4% ice-cold paraformaldehyde for 24 hours and decalcified with 19% EDTA (Sigma-Aldrich Corp.) for 14 days prior to paraffin embedding. Hematoxylin and eosin (H&E) staining was performed on 5-µm sections. Images were documented by a Keyence BZ-X710 system (Itasca, IL, USA). IHC staining was performed on 5-µm deparaffinized sections with the same antibodies used for ICC staining.

Duolink® proximity ligation assay (PLA)

All reagents used for the Duolink® PLA assay were purchased from Sigma-Aldrich Corp. Deparaffinized sections were blocked with Duolink® blocking solution at room temperature for one hour before incubation with the same primary antibodies used in IHC staining, but diluted in Duolink® antibody diluent at 4°C overnight. The following day, the sections were washed, and then incubated with Duolink® In Situ PLA® Probe Anti-Rabbit MINUS and Probe Anti-Goat PLUS (for Cntnap4 and Cntnap3), or Probe Anti-Rabbit MINUS and Probe Anti-Mouse PLUS (for Cntnap2) at 37°C for 60 min, following manufacturer instructions. Amplification solution was mixed with polymerase and applied to the slides for 100 min at 37°C, accordingly. The slides were washed, mounted with Duolink® In Situ Mounting Medium with DAPI, and examined with Leica TCS SP8 Confocal Laser Scanning Platform.

RNA interference (RNAi)

MC3T3-E1 and ADTC5 cells were transfected with *Cntnap4* shRNA Lentiviral particles (Santa Cruz Biotechnology, Santa Cruz, CA, USA) or non-target control shRNA by Lipofectamine® 3000. The positive transfected colonies were selected by Puromycin (Sigma-Aldrich Corp.) and validated by *Cntnap4* mRNA expression levels to establish the *Cntnap4* knockdown cell line.

In vitro osteogenic differentiation assays

Control and stable *Cntnap4*-KD MC3T3-E1 cells were seeded on 24-well plates for alkaline phosphatase (ALP), Alizarin Red, and immunocytochemistry (ICC) staining. In addition, cells were seeded on 6-well plates for the osteogenic genes expression assay. Both cell types were cultured in osteogenic differentiation medium [α-MEM, 10% fetal bovine serum (FBS; Thermo Fisher Scientific), 50 μg/ml ascorbic, and 10 mM β-glycerophosphate (Sigma-Aldrich Corp.)] with or without 500 ng/ml Nell-1 or 100 ng/ml BMP2 (Medtronic, Minneapolis, MN, USA). The specific PCR primer sets used for real-time PCR analysis and the primary antibodies used for staining are listed in **Tables 2 and 3**, respectively.

Western blot

Sub-confluent control and *Cntnap4*-KD MC3T3-E1 cells were subjected to serum starvation for 18 hours before PBS control or 500 ng/ml Nell-1 treatment. Protein isolation and Western blot were performed as previously described (33). Primary antibodies are listed in **Table 3**.

Behavioral phenotyping assays for mouse models of autism

Conventional phenotyping assays for mouse models of autism were employed using adult *Nell-1*$^{+/-}$ and wildtype mice. Repetitive behaviors were assessed by the over-grooming test (34) and the marble-burying test (35) as previously described. Abnormal social interactions were assessed using the three chambers social behavioral test as previously described (36).

Statistical analysis

All statistical analyses were conducted in consultation with the UCLA Statistical Biomathematical Consulting Clinic. Initial sample numbers were determined using a power analysis to give α = 0.05 and power = 0.8. Statistical significance was performed with OriginPro 8 (Origin Lab Corp., Northampton, MA, USA) and included the one-way ANOVA and two-sample *t*-test. Individual comparisons between two groups were determined by the Mann-Whitney test for non-parametric data. Statistical significance was determined at the $P < 0.05$ level.

Results

T7 phage particles with 1st and 2nd Cntnap4 LamG extracellular domains exhibit high binding affinity to Nell-1

A biopanning approach was utilized to identify potential native binding protein(s) of Nell-1. Specifically, a human brain cDNA library was used to construct a T7 phage display cDNA library. The phages bound to the His-tagged Nell-1 coated beads were eluted after four rounds of biopanning. One hundred plaques were subsequently selected for phage DNA amplification by PCR, and all resultant DNA fragments over 500 bp in size were sequenced (**Figure 1**). In total, twenty-three Nell-1-binding candidate proteins were isolated, of which nine were found to be transmembrane proteins (**Table 4**). In particular, phage particles harboring a sequence that aligned with the first and second LamG extracellular domains of Cntnap4 were detected repeatedly when using the Basic Local Alignment Search Tool (BLAST) (**Figure 2A**). These phage sequences exhibited high binding affinities to full-length Nell-1 protein (**Figure 2B, C**). Deletion of the Nell-1 LamG domain virtually eradicated the binding of the Cntnap4 phage to Nell-1, suggesting that the N-terminal LamG domain is critical for the ligand-receptor-like interaction between Nell-1 and Cntnap4 (**Figure 2C, D**).

Nell-1 and Cntnap4 bind on the plasma membrane of osteogenic-committed cells

Among the eight Nell-1-responsive cell lines used for Cntnap4 expression screening (**Table 1**), the osteogenic-committed MC3T3-E1 cell line (37, 38) exhibited the highest levels of *Cntnap4* expression (**Figure 3A**). On the other hand, the less differentiated cell lines [C3H10T1/2, ST-2, 143B, MG63, and SaoS2 (37, 39-42)], the predominantly adipogenic-committed cell line [M2-10B4 (43)], and the chondrogenic-committed cell line [ATDC5 (44)] exhibited relatively lower

levels of *Cntnap4* expression (**Figure 3A**). Among the four types of tested primary cells, the primary newborn mouse calvaria cells (NMCCs), which are known to demonstrate great osteogenic capability (6), exhibited the highest levels of *Cntnap4* expression (**Figure 3B**). In fact, primary NMCCs had significantly higher levels of Cntnap4 expression than mouse rib chondrocytes, human articular chondrocytes, and human bone marrow stem cells (**Figure 3B**). Moreover, exogenous administration of Nell-1 significantly upregulated *Cntnap4* expression in MC3T3-E1 pre-osteoblasts and primary NMCCs (data not shown).

Confocal laser scanning microscopy of the samples incubated with exogenous recombinant human Nell-1 confirmed co-localization of Nell-1 and Cntnap4 on the plasma membrane of MC3T3-E1 and primary NMCCs (**Figure 4A, B**). These results were further validated with an *in situ* Duolink® proximity ligation assay, confirming direct Nell-1 and Cntnap4 interaction on the plasma membrane of both MC3T3-E1 and primary NMCCs (**Figure 4 A, B**).

Cntnap4 knockdown reduces Nell-1-responsive osteogenesis

In determining whether Cntnap4 is essential for Nell-1-mediated osteogenesis, stable *Cntnap4*-knockdown (*Cntnap4*-KD) MC3T3-E1 cells were established using *Cntnap4* small hairpin RNA (shRNA) and subsequently treated with a PBS control, Nell-1 protein, or BMP2. Treatment of control scramble-shRNA transfected MC3T3-Ef1 cells with Nell-1 protein markedly increased alkaline phosphatase (ALP) and Alizarin Red staining, while only negligible staining was detected in Nell-1 treated *Cntnap4*-KD MC3T3-E1 cells (**Figure 5A**). On the other hand, treatment of control MC3T3-E1 cells and *Cntnap4*-KD MC3T3-E1 cells with BMP2, an osteogenic protein with a signaling pathway distinct from Nell-1 (1), resulted in similar robust osteogenic responses (**Figure 5A**). These data intimate that *Cntnap4*-KD specifically targets Nell-1, but not BMP2-

mediated MC3T3-E1 cell osteogenic differentiation. In addition, Nell-1 protein significantly enhanced osteocalcin (Ocn) and osteopontin (Opn) expression in control MC3T3-E1 pre-osteoblasts as evidenced by positive staining; however, this effect was not observed in Nell-1 treated *Cntnap4*-KD MC3T3-E1 cells (**Figure 5B**). Moreover, treatment with Nell-1 protein resulted in increased concomitant gene expression of the osteogenic markers *Alp*, *Collagen Iα1*, *Collagen Iα2*, *Ocn*, *Opn*, and *bone sialoprotein (Bsp)* in control MC3T3-E1 cells, but did not increase gene expression of the same markers in *Cntnap4*-KD MC3T3-E1 cells (**Figure 5C**). In sum, these data indicate that Cntnap4 is critical for Nell-1 osteogenic bioactivity.

Cntnap4 mediates Nell-1-activated MAPK and Wnt signaling in osteogenic-committed cells

Because *Cntnap4*-KD resulted in a reduced osteogenic response of MC3T3-E1 cells to Nell-1 but not to BMP2, this suggests the specific involvement of Cntnap4 in osteogenesis as regulated by Nell-1. Consequently, the effect of *Cntnap4*-KD on the Wnt and MAPK signaling pathways during osteogenic differentiation was investigated due to the fact that Nell-1 is a known activator of Wnt and MAPK transduction during osteogenesis (11, 33, 45, 46). Although Nell-1 stimulation induced high levels of ERK and JNK phosphorylation in control MC3T3-E1 pre-osteoblasts, it did not alter the expression levels of ERK and JNK phosphorylation in *Cntnap4*-KD MC3T3-E1 cells (**Figure 6A**). In a similar vein, while Nell-1 treatment significantly increased both intracellular and nuclear levels of Axin2 and active β-catenin in control MC3T3-E1 cells, *Cntnap4*-KD resulted in complete elimination Nell-1-responsive Wnt signaling (**Figure 6B, C**). Taken together, these findings point to the fact that Cntnap4 is not only essential, but also specific for Nell-1 activation of the MAPK and Wnt signaling pathways in osteogenic-committed cells.

Discussion

In our search to find a specific cell surface receptor for Nell-1-mediated osteogenesis, we unexpectedly identified Cntnap4, a plasma membrane protein, to bind to Nell-1 with high-binding affinity. Due to the fact that Cntnap4 is a neurexin superfamily protein member belonging to a large category of synaptic cell adhesion molecules with important roles in connecting pre- and post-synapses critical to synapse development and cortical interneuron function (27, 28, 30), its novel discovery as a specific cell membrane receptor for Nell-1 in osteogenic-committed cells was surprising. Nonetheless, this unanticipated discovery connecting Cntnap4 to osteogenesis with Nell-1 serving as a ligand of Cntnap4 provides a foundational framework for further exploration of the Nell-1/Cntnap4 functional axis. Specifically, this novel interaction merits additional investigation into its potential effects on skeletal function and possibly neuronal function as well.

Supporting the notion that the Nell-1/Cntnap4 functional axis may be involved in neural development, we have observed neurologic anomalies in addition to osseous anomalies in Nell-1 gain- and loss-of-function mouse models. For example, overexpression of Nell-1 in mice results in a multitude of anomalies ranging from craniosynostosis to neural tube defect acrania (47) – a rare human congenital disease that is often associated with exencephaly (48). On the other hand, Nell-1 deficient mice exhibit calvarial defects closely resembling the defects seen in patients with cleidocranial dysplasia (CCD) (7). Despite the fact that *Cntnap4-eGFP* knock-in and knock-out mice are viable without grossly apparent calvarial defects (28), it is possible that skeletal abnormalities may be overlooked in Cntnap4-deficient mouse models. As can be seen, Nell-1 transgenic mouse models demonstrate incomplete perinatal penetrance of calvarial bone disorders, suggesting a similar manifestation in Cntnap4-deficient mouse models. Accordingly, our novel

findings invite future research using *Cntnap4-null* and *Cntnap4-overexpression* animal models to fully investigate the role of Cntnap4 in skeletal development and regeneration.

Although previous attempts to search for a Nell-1 specific cell surface receptor have been unsuccessful, Nell-1 has been shown to bind other intracellular molecules with less specificity. For instance, all-trans retinoic acid induced differentiation factor (ATRAID, also known as apoptosis-related protein 3, APR3) was previously detected as an intracellular Nell-1 binding protein by using a T7 Saos2 cDNA library (32). However, because ATRAID is a protein found mainly on the lysosomal membrane (50), it is reasonably unlikely to be a candidate for extracellular Nell-1 binding and signal transduction. Rather, due to the similarities ATRAID shares with lysosome-associated membrane protein 1 and 2 (Lamp-1 and Lamp-2) (50), it is more likely to play a role in endocytosis or transportation of Nell-1. In fact, this rationale may explain our previous finding that ATRAID can bind with multiple truncated Nell-1 constructs with or without the N-terminal LamG domain (32). Besides ATRAID, integrin-β1 has also been reported to bind Nell-1 (51, 52). That being said, integrin-β1 has been demonstrated to bind promiscuously with a wide range of molecules and is therefore not Nell-1-specific (51, 53, 54). Structurally, whereas integrin-β1 binds to the C-terminus of Nell-1(51), in this paper we found that Cntnap4 binds to the N-terminus of Nell-1 (**Figure 2**). As such, this raises the possibility for potential interplay between integrin-β1 and Cntnap4-mediated Nell-1-responsive signal transduction.

When elucidating a potential connection between Cntnap4 and the Nell-1 signaling pathway during osteogenesis, it is crucial to consider how they relate to the Wnt and MAPK signaling pathways (11, 33, 45, 46). Because *Cntnap4* knockdown resulted in a reduced osteogenic response of MC3T3-E1 cells to Nell-1 but not to BMP2, this suggests that *Cntnap4*-KD specifically targets Nell-1 and not BMP-2 mediated osteogenic differentiation (**Figure 5**). In the

present study, we demonstrated that Cntnap4 is essential and specific for Nell-1 activation of the MAPK and Wnt signaling pathways in osteogenic-committed cells (**Figure 6**). As a result, the likely pathway is as follows: as a secreted molecule, Nell-1 initiates the cellular signaling process through binding on the cell surface to its specific receptor, Cntnap4. Nell-1 then activates ERK and JNK in MAPK signaling, and also promotes the phosphorylation of Runx2. This, in turn, stimulates expression of Nell-1 and Ocn by binding directly to their promoters. In addition, once again through binding on the cell surface to Cntnap4, Nell-1 simultaneously promotes the expression of Axin2 and active β-catenin, thus increasing nuclear translocation of active β-catenin.

While the influence of the central nervous system on bone development and morphogenesis is widely recognized, recent studies suggest that the skeleton also orchestrates the development and cognitive functions of the nervous system (55-58). To this end, although previous Nell-1 studies have focused primarily on the skeletal system, Nell-1 was first identified in both the fetal and adult human brain (2) with abundant *Nell-1* expression detected in developing and adult nervous systems (24). Importantly, Nell-1 and Cntnap4 display largely overlapping spatial expression patterns in the hippocampus, inferior olivary nucleus, and spinal cord (24, 27, 59).

Interestingly, transcriptome analyses implicate both *Nell-1* and *Cntnap4* in several neurodegenerative and neuropsychiatric disorders such as ASD and Alzheimer's disease (60-62), furthering the notion of a Nell-1/Cntnap4 functional axis. Similarly, our preliminary studies revealed that *Nell-1*-mutant mice exhibit aberrant and repetitive behaviors, as seen in *Cntnap4*-mutant mice (28). It is worth noting that some young CCD patients have delayed motor skill development such as crawling and walking (63), developmental skill milestones associated with multiple brain areas. Furthermore, in addition to physical development delays, some CCD patients also exhibit cognitive disorders (64). Consequently, the possibility of replicating the described

cognitive disorders of CCD patients in Nell-1/Cntnap4 deficient models is of profound clinical interest with significant implications in neuroskeletal syndromes. As a result, further exploration is warranted to determine whether the functional involvement of the Nell-1/Cntnap4 axis is as active in neural tissues as it is in skeletal tissues. Looking ahead, the Nell-1/Cntnap4 functional axis may provide a novel framework for future mechanistic studies in neuroskeletal biology during development and homeostasis, as well as in health and disease.

Conclusion

In the present study, we identified and validated Cntnap4 as the first specific cell surface receptor of Nell-1. In particular, we demonstrated that: 1) Nell-1 and Cntnap4 co-localize on the surface of osteogenic-committed cells, 2) Nell-1 and Cntnap4 exhibit high-affinity interactions, 3) Cntnap4 knockdown reduces Nell-1-responsive osteogenesis, and 4) Cntnap4 mediates Nell-1-activated MAPK and Wnt signaling in osteogenic-committed cells. The unexpected discovery of the ligand-receptor-like interaction between Nell-1 and Cntnap4 during osteogenesis provides a foundational framework for further exploration of a novel functional axis as it relates to skeletal and potential neuronal function. Looking ahead, these exciting findings pave the way for future studies that may provide not only innovative insight into the role of Nell-1 in the nervous system, but also mechanistic insight into the role of the Nell-1/Cntnap4 functional axis in neuroskeletal interplay and crosstalk.

Table 1. Cell lines and primary cells used for Cntnap4 expression screening.

	Cell Type	Species	Source
cell line	C3H10T1/2 (Clone 8: ATCC® CCL-226™)	mouse	embryo/sarcoma
	M2-10B4 (ATCC® CRL-1972™)	mouse	bone marrow/stroma
	MC3T3-E1 (Subclone 4: ATCC® CRL-2593™)	mouse	calvaria
	ST-2 (DSMZ ACC 333)	mouse	bone marrow/stroma
	ATDC5 (HPA 99072806)	mouse	teratocarcinoma
	143B (ATCC® CRL-8303™)	human	osteosarcoma
	SaoS2 (ATCC® HTB-85™)	human	osteosarcoma
	MG63 (ATCC® CRL-1427™)	human	osteosarcoma
primary cell	newborn mouse calvaria cells (NMCC)	mouse	calvaria
	mouse rib chondrocytes (mRC)	mouse	rib cage
	human articular chondrocytes (hARC)	human	articular cartilage
	human bone marrow stromal cells (hBMSC)	human	bone marrow

Table 2. Primer and probe sets used for real-time PCR.

TaqMan® primer and probe sets (Thermo Fisher Scientific)		
Species	**Gene**	**Assay ID**
Human	*Gapdh*	Hs02786624_g1
Human	*Cntnap4*	Hs00369159_m1
Mouse	Gapdh	Mm99999915_g1
Mouse	*Cntnap4*	Mm00519175_m1
Mouse	*Cntnap3*	Mm01297195_m1
Mouse	*Cntnap2*	Mm00470553_m1

Power SYBR Green PCR Master Mix primers (Thermo Fisher Scientific)		
Species	**Gene**	**Primer sequence**
Mouse	*Alp*	5’ - ACT GAT GTG GAA TAC GAA CTG GAT GAG AAG G - 3’ 5’ - CAG TCA GGT TGT TCC GAT TCA ATT CAT ACT GC - 3’
Mouse	*Col Iα1*	5’ - CTG GCG GTT CAG GTC CAA T - 3’ 5’ - TTC CAG GCA ATC CAC GAG C - 3’
Mouse	*Col Iα2*	5’ - AAG GGT GCT ACT GGA CTC CC - 3’ 5’ - TTG TTA CCG GAT TCT CCT TTG G - 3’
Mouse	*Ocn*	5’ - CTG CCC TAA AGC CCA AAC TCT - 3’ 5’ - GAG AGG ACA GGG AGG ATC AA - 3’
Mouse	*Opn*	5’ - AGC AAG AAA CTC TTC CAA GCA A - 3’ 5’ - GTG AGA TTC GTC AGA TTC ATC CG - 3’
Mouse	*BSP*	5’ - ATG GAG ACG GCG ATA GTT CC - 3’ 5’ - CTA GCT GTT ACA CCC GAG AGT - 3’
Mouse	*Nfatc2*	5’ - CTT TCA GAT GGG AAT AAA CGT C - 3’ 5’ - TCC TAC TCA CAT AGC, AAC AGA A - 3’
Mouse	*Gapdh*	5’ - ATT CAA CGG CAC ATG CAA GG - 3’ 5’ - GAT GTT AGT GGG GTC TCG CTC - 3’

Table 3. Primary antibodies used for immunohistochemistry staining and Western blot analysis.

Target	Application	Dilution	Supplier
Cntnap4	Staining	1:200	Santa Cruz Biotechnology
Cntnap3	Staining	1:50	Santa Cruz Biotechnology
Cntnap2	Staining	1:50	Abcam
Nell-1	Staining	1:75	Allele Biotech
Ocn	Staining	1:200	Santa Cruz Biotechnology
Opn	Staining	1:200	Santa Cruz Biotechnology
ERK1+ERK2	Western	1:1,000	Abcam
ERK1 (phospho Y204) + ERK2 (phospho Y187)	Western	1:1,000	Abcam
JNK1	Western	1:1,000	Abcam
JNK1 + JNK2 + JNK3 (phospho Y185 + Y185 + Y223)	Western	1:1,000	Abcam
p38	Western	1:1,000	Abcam
p38 (phospho T180 + Y182)	Western	1:1,000	Abcam
Active-β-catenin	Western	1:5,000	EMD Millipore
β-Catenin	Western	1:1,000	Abcam
Axin2	Western	1:1,000	Abcam
Nell-1	Western	1:500	Allele Biotech
Cntnap4	Western	1:500	Sigma-Aldrich
Actin	Western	1:500	Santa Cruz Biotechnology
Histone H3	Western	1:1,000	EMD Millipore

Table 4. Nell-1-binding candidate proteins screened by phage biopanning.

Transmembrane Proteins	
Protein	**Gene**
Amyloid beta A4 protein	*App*
Annexin A13	*Anxa13*
Contactin-associated protein-like 4	*Cntnap4*
FXYD domain-containing ion transport regulator 6	*Fxyd6*
Myelin basic protein	*Mbp*
Reticulon-3	*Rtn3*
Toll-like receptor 7	*Tlr7*
Suppressor of tumorigenicity 7 protein-like	*St7l*
Vesicular glutamate transporter 1	*Slc17a7*

Others	
Protein	**Gene**
ATP-dependent RNA helicase DDX42 (EC 3.6.4.13) (DEAD box protein 42)	*Ddx42*
Cholecystokinin	*Cck*
DUSP 16 protein	*Dusp16*
E3 ubiquitin-protein ligase NEDD4-like	*Nedd4l*
Epidermal growth factor-like protein 7	*Efgl7*
Eukaryotic translation initiation factor 2 subunit 3	*Eif2s3*
Formin-binding protein 4	*Fnbp4*
Hypermethylated in cancer 2 protein	*Hic2*
Nicotinamide mononucleotide adenylyltransferase 2	*Nmnat2*
Pre-B-cell leukemia transcription factor interacting protein 1	*Pbxip1*
Proactivator polypeptide	*Psap*
Protein phosphatase 1 regulatory subunit 14A	*Ppp1r14a*
S-phase kinase-associate protein 1	*Skp1*
Tropomodulin 3	*Tmod3*

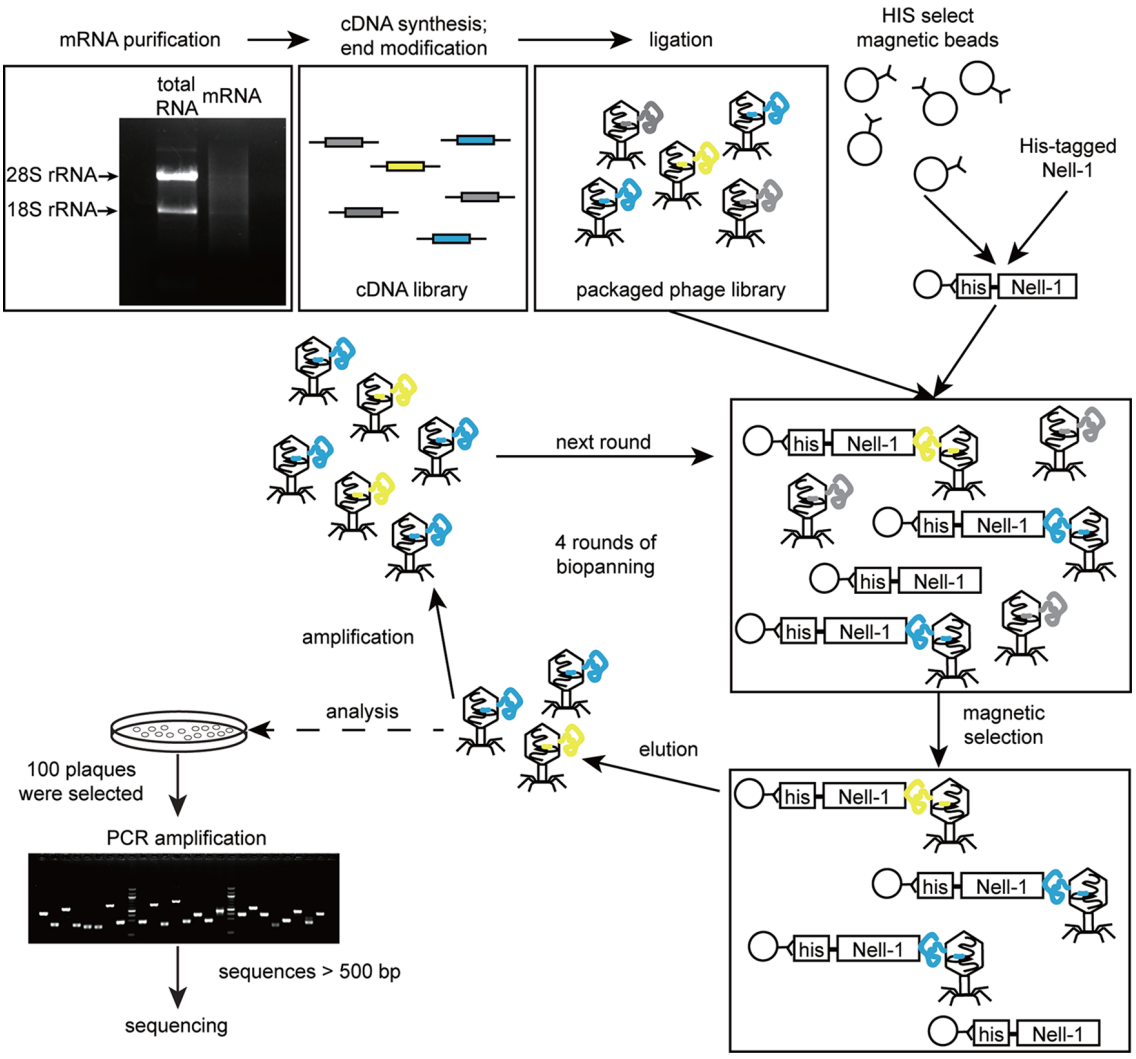

Figure 1. Schematic of phage biopanning. A cDNA library was constructed from human brain mRNA, packaged with T7 phages, and subsequently probed with His-tagged Nell-1-coated magnetic beads. The phages bound to the His-tagged Nell-1 coated beads were eluted after four rounds of biopanning. One hundred plaques were subsequently selected for phage DNA amplification by PCR. Resultant DNA fragments over 500 bp in size were sequenced and considered binding candidates.

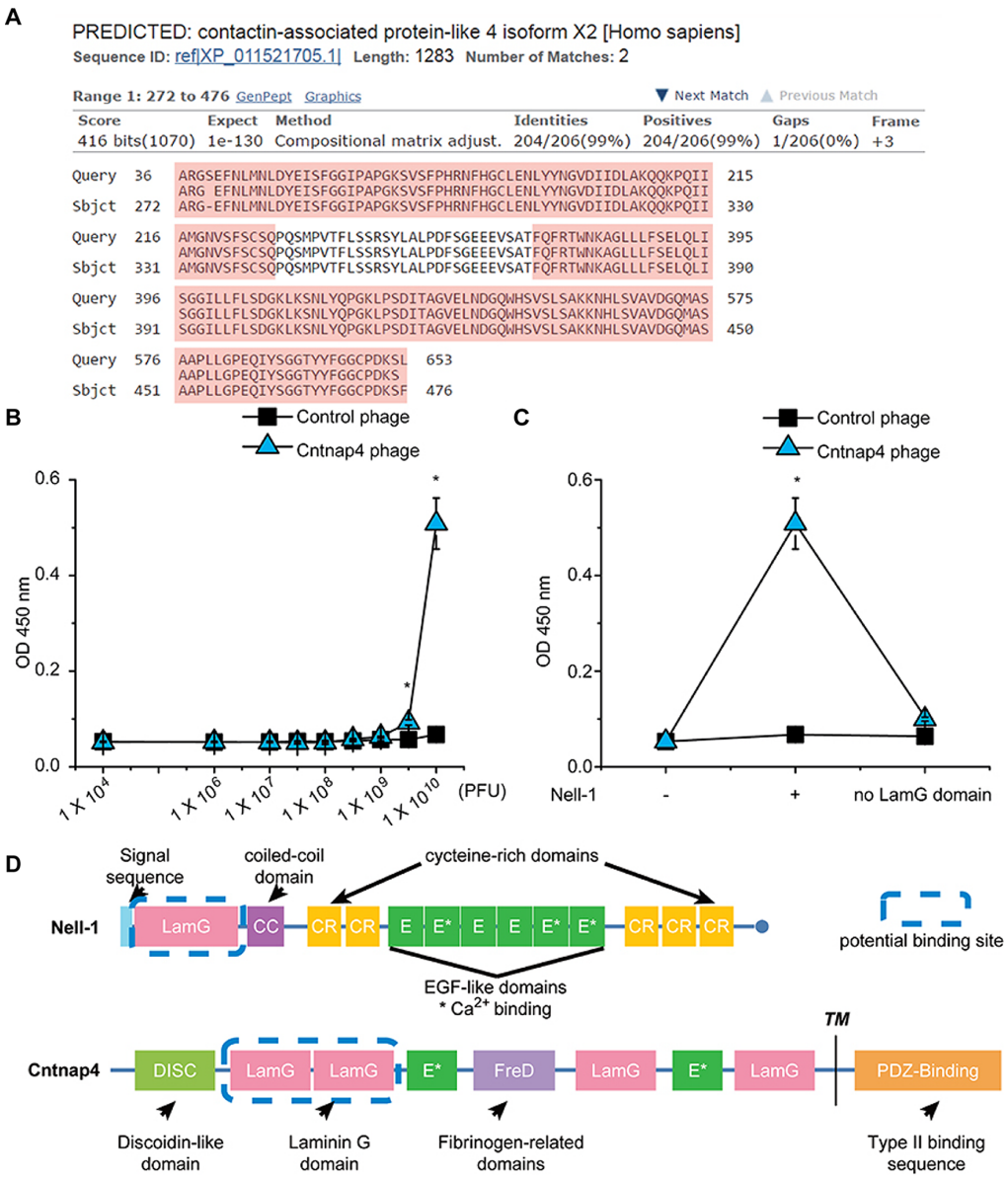

Figure 2. Binding affinity confirmation between Cntnap4 phages and Nell-1. (**A**) The Basic Local Alignment Search Tool (BLAST) result of the T7 phage amino acid sequence matched with the human Cntnap4 partial protein sequence. Query: the amino acid sequence of the phage particles; Sbjct: the matching Cntnap4 amino acid sequence. LamG domains are highlighted in pink. (**B**) The Cntnap4 phage exhibited a significantly greater binding affinity than the control phage when increasing the number of phages incubated with Nell-1 pre-coated ELISA plates. (**C**)

The Cntnap4 phage exhibited high binding affinity to full-length Nell-1. Deletion of the Nell-1 LamG domain virtually eliminated binding of the Cntnap4 phage to Nell-1. (**D**) The structure of Nell-1 and Cntnap4 and their potential binding site. Nell-1 is a secreted protein of 810 amino acids and contains an N-terminal laminin G (LamG) domain, a coiled-coil (CC) domain, five cysteine-rich (CR) domains, and six epidermal growth factor (EGF)-like repeats. Cntnap4 is a transmembrane protein of 1310 amino acids and contains a large extracellular domain, a single transmembrane domain, and a short cytoplasmic region. The extracellular region of Cntnap4 consists of a discoidin-like domain (DISC), four LamG domains, a fibrinogen-related domain (FreD), and two EGF repeats, while the cytoplasmic region contains a binding site for PDZ domains. The potential binding domain of Nell-1 and Cntnap4 is highlighted by the blue dashed line. TM: transmembrane. Mean ± SEM of six independent experiments performed in triplicate are shown. *: $P < 0.05$.

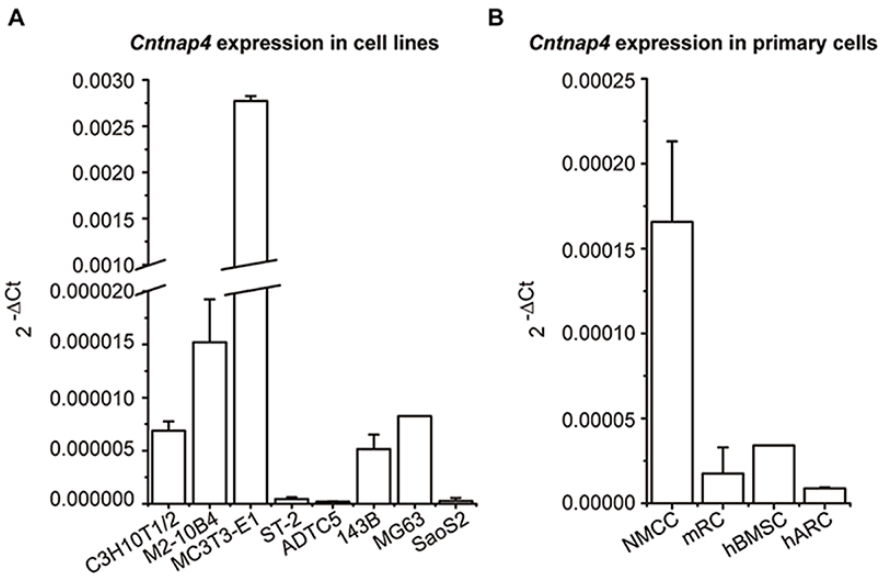

Figure 3. Cntnap4 mRNA expression levels in twelve types of non-neuron and glial cells. **(A)** Among the eight Nell-1-responsive cell lines used for Cntnap4 expression screening, the osteogenic-committed MC3T3-E1 cell line exhibited the highest levels of *Cntnap4* expression. **(B)** Among the four types of tested primary cells, the primary newborn mouse calvaria cells exhibited the highest levels of *Cntnap4* expression NMCC: newborn mouse calvarial cells. mRC: mouse rib chondrocytes. hBMSC: human bone marrow stem cells. hARC: human articular chondrocytes. Mean ± SEM of six independent experiments performed in triplicate are shown.

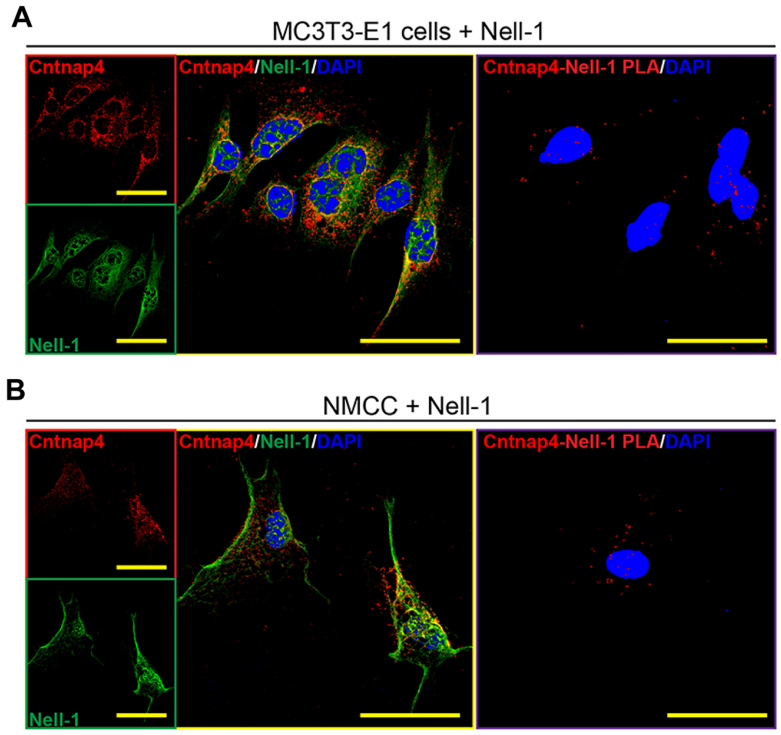

Figure 4. Cntnap4 and Nell-1 co-localize on the surface of osteogenic-committed cells and in mouse calvarial bone. (A) Confocal laser scanning microscopy of the samples incubated with exogenous recombinant human Nell-1 visualized co-localization of Nell-1 and Cntnap4 on the plasma membrane of MC3T3-E1 pre-osteoblasts. Findings were validated with an *in situ* Duolink® proximity ligation assay. **(B)** Similarly, Nell-1 and Cntnap4 co-localization was confirmed on the plasma membrane of primary NMCC after incubation with exogenous recombinant human Nell-1. Findings were validated with an *in situ* Duolink® proximity ligation assay. Scale bar = 50 μm (yellow).

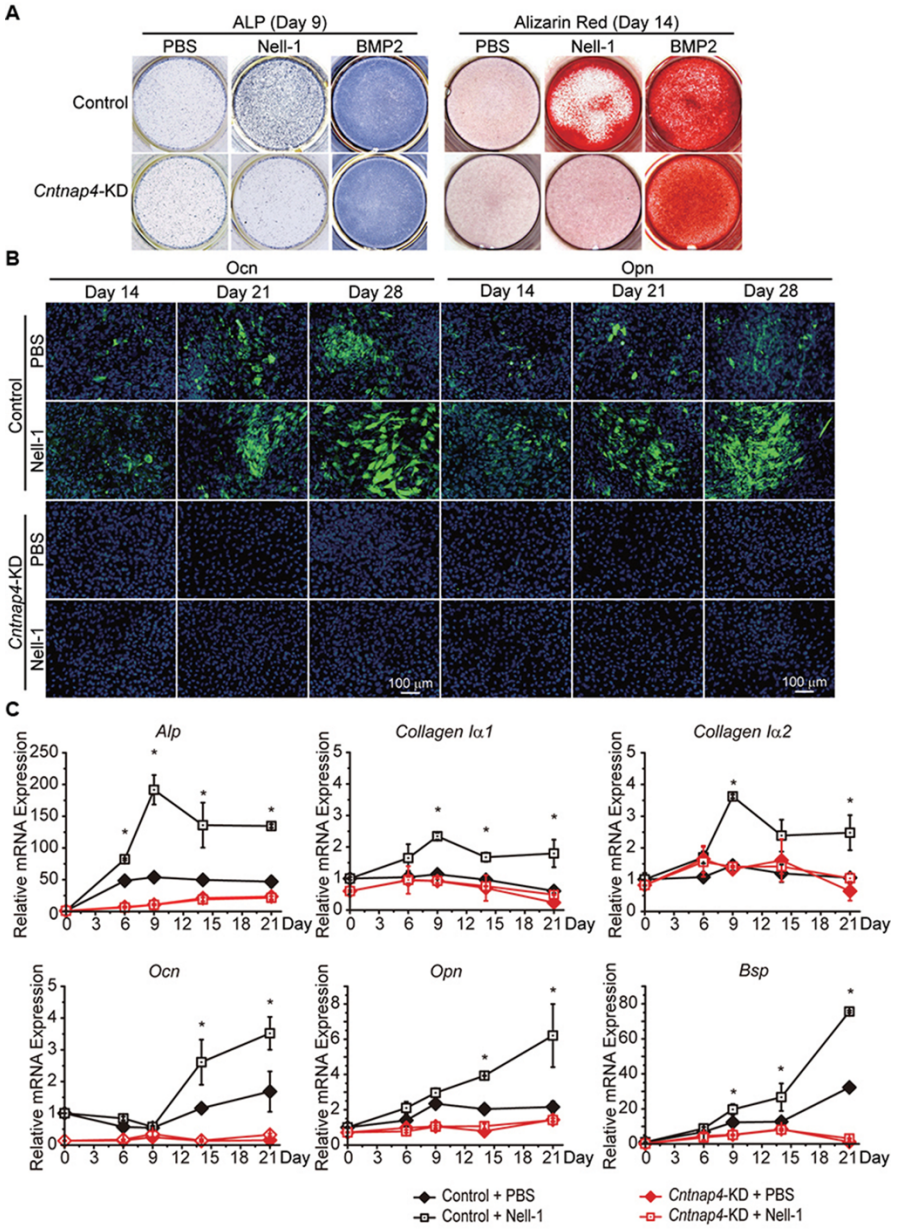

Figure 5. Cntnap4 is essential for Nell-1 osteogenic bioactivity *in vitro*. (A) To determine whether Cntnap4 is essential for Nell-1-mediated osteogenesis, stable *Cntnap4*-KD MC3T3-E1 cells were established using *Cntnap4* small hairpin RNA and treated with a PBS control, Nell-1 protein, or BMP2. Both Nell-1 and BMP2 treatment increased alkaline phosphatase (ALP) staining on day 9 and Alizarin Red staining on day 14 in control shRNA transfected MC3T3-E1 cells,

whereas only BMP2 increase staining intensity in *Cntnap4*-KD MC3T3-E1 cells. **(B)** Nell-1 protein administration significantly enhanced osteocalcin (Ocn) and osteopontin (Opn) staining in a time-dependent fashion in control MC3T3-E1 cells, more so than PBS administration at each time point. Neither Ocn nor Opn staining was observed in Nell-1 or PBS treated *Cntnap4*-KD MC3T3-E1 cells. (**C**) Nell-1 protein resulted in significant peak expression levels of *Alp*, *Collagen Iα1*, and *Collagen Iα2* 9 days after administration in control MC3T3-E1 cells, whereas *Ocn*, *Opn*, and *Bsp* presented significant time-dependent patterns of increased gene expression. Nell-1 stimulation did not result in increased gene expression of the same osteogenic markers in *Cntnap4*-KD MC3T3-E1 cells. Mean ± SEM of six independent experiments performed in triplicate are shown. *: $P < 0.05$ when compared to the Control + PBS group. Scale bar = 100 μm.

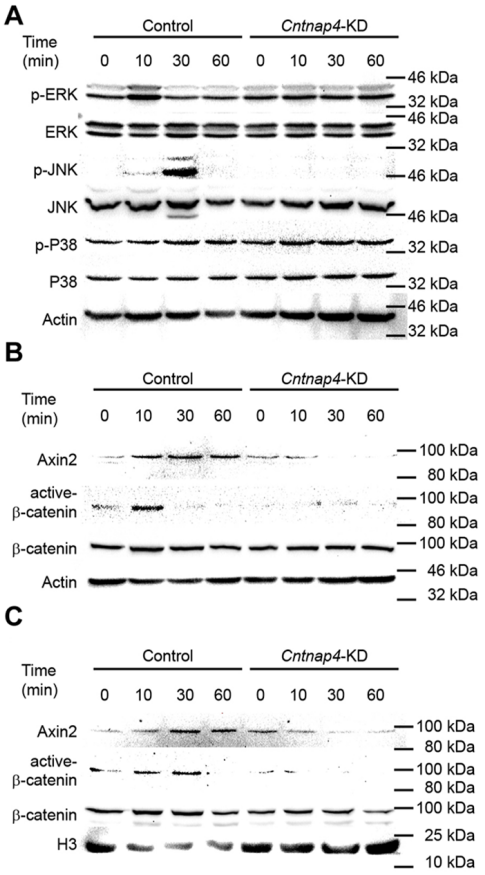

Figure 6. Cntnap4 is essential for Nell-1-activated MAPK and Wnt signaling *in vitro*. (**A**) The effect of *Cntnap4*-KD on the Wnt and MAPK signaling pathways during osteogenic differentiation was investigated. In control MC3T3-E1 pre-osteoblasts, significantly higher levels of pERK and pJNK were detected 10 min and 30 min after Nell-1 stimulation, respectively, while no changes were detected in P38 expression levels. On the other hand, Nell-1 stimulation did not alter the expression levels of pERK and pJNK in *Cntnap4*-KD MC3T3-E1 cells. The expression levels of Wnt signaling molecules in (**B**) the whole cell lysate and (**C**) the cell nuclear lysate of control and *Cntnap4*-KD MC3T3-E1 cells were also investigated. While Nell-1 treatment significantly

increased both intracellular and nuclear levels of Axin2 and active β-catenin in control MC3T3-E1 cells, *Cntnap4*-KD resulted in complete elimination Nell-1-responsive Wnt signaling.

References

1. Zhang X, Zara J, Siu RK, Ting K, Soo C. The role of NELL-1, a growth factor associated with craniosynostosis, in promoting bone regeneration. *Journal of dental research* 2010 Sep; **89**(9)**:** 865-878.

2. Watanabe TK, Katagiri T, Suzuki M*, et al.* Cloning and characterization of two novel human cDNAs (NELL1 and NELL2) encoding proteins with six EGF-like repeats. *Genomics* 1996 Dec 15; **38**(3)**:** 273-276.

3. Ting K, Vastardis H, Mulliken JB*, et al.* Human NELL-1 expressed in unilateral coronal synostosis. *Journal of bone and mineral research : the official journal of the American Society for Bone and Mineral Research* 1999 Jan; **14**(1)**:** 80-89.

4. Zhang X, Carpenter D, Bokui N*, et al.* Overexpression of Nell-1, a craniosynostosis-associated gene, induces apoptosis in osteoblasts during craniofacial development. *Journal of bone and mineral research: the official journal of the American Society for Bone and Mineral Research* 2003 Dec; **18**(12)**:** 2126-2134.

5. Desai J, Shannon ME, Johnson MD*, et al.* Nell1-deficient mice have reduced expression of extracellular matrix proteins causing cranial and vertebral defects. *Human molecular genetics* 2006 Apr 15; **15**(8)**:** 1329-1341.

6. Truong T, Zhang X, Pathmanathan D, Soo C, Ting K. Craniosynostosis-associated gene nell-1 is regulated by runx2. *Journal of bone and mineral research: the official journal of the American Society for Bone and Mineral Research* 2007 Jan; **22**(1)**:** 7-18.

7. Zhang X, Ting K, Pathmanathan D*, et al.* Calvarial cleidocraniodysplasia-like defects with ENU-induced Nell-1 deficiency. *The Journal of craniofacial surgery* 2012 Jan; **23**(1)**:** 61-66.

8. Huang DW, Sherman BT, Lempicki RA. Systematic and integrative analysis of large gene lists using DAVID bioinformatics resources. *Nat Protoc* 2009; **4**(1)**:** 44-57.

9. Li W, Zara JN, Siu RK*, et al.* Nell-1 enhances bone regeneration in a rat critical-sized femoral segmental defect model. *Plastic and reconstructive surgery* 2011 Feb; **127**(2)**:** 580-587.

10. Aghaloo T, Cowan CM, Chou YF*, et al.* Nell-1-induced bone regeneration in calvarial defects. *The American journal of pathology* 2006 Sep; **169**(3)**:** 903-915.

11. James AW, Shen J, Zhang X*, et al.* NELL-1 in the treatment of osteoporotic bone loss. *Nature communications* 2015; **6:** 7362.

12. Shen J, James A, Khadarian K*, et al.* Nell-1 promotes spinal fusion in non-human primates. Orthopaedic Research Society (ORS) 2015 Annual Meeting; 2015 Mar 28 - 31, 2015; Las Vegas, Nevada Orthopaedic Research Society; 2015. p. 1577.

13. Siu RK, Lu SS, Li W*, et al.* Nell-1 protein promotes bone formation in a sheep spinal fusion model. *Tissue engineering Part A* 2011 Apr; **17**(7-8)**:** 1123-1135.

14. Jin Z, Mori Y, Yang J*, et al.* Hypermethylation of the nel-like 1 gene is a common and early event and is associated with poor prognosis in early-stage esophageal adenocarcinoma. *Oncogene* 2007 Sep 20; **26**(43)**:** 6332-6340.

15. Zhang X, Kuroda S, Carpenter D*, et al.* Craniosynostosis in transgenic mice overexpressing Nell-1. *The Journal of clinical investigation* 2002 Sep; **110**(6)**:** 861-870.

16. James AW, Pan A, Chiang M*, et al.* A new function of Nell-1 protein in repressing adipogenic differentiation. *Biochemical and biophysical research communications* 2011 Jul 22; **411**(1)**:** 126-131.

17. Xue J, Peng J, Yuan M*, et al.* NELL1 promotes high-quality bone regeneration in rat femoral distraction osteogenesis model. *Bone* 2011 Mar 1; **48**(3)**:** 485-495.

18. Shen J, James AW, Zara JN*, et al.* BMP2-Induced Inflammation Can Be Suppressed by the Osteoinductive Growth Factor NELL-1. *Tissue Eng Pt A* 2013 Nov 1; **19**(21-22)**:** 2390-2401.

19. Shen J, James AW, Zhang X*, et al.* Novel Wnt Regulator NEL-Like Molecule-1 Antagonizes Adipogenesis and Augments Osteogenesis Induced by Bone Morphogenetic Protein 2. *The American journal of pathology* 2016 Feb; **186**(2)**:** 419-434.

20. Batra, J., Robinson, J., Mehner, C., Hockla, A., Miller, E., Radisky, D.C., and Radisky, E.S. PEGylation extends circulation half-life while preserving in vitro and in vivo activity of tissue inhibitor of metalloproteinases-1 (TIMP-1). *PLoS One* 2012 November; **7**(11): e50028.

21. Dozier, J.K., andDistefano, M.D. Site-Specific PEGylation of Therapeutic Proteins. Int J Mol Sci 2015 Oct; **16**(10): 25831-25864.

22. Huang, Z., Zhu, G., Sun, C., Zhang, J., Zhang, Y., Zhang, Y., Ye, C., Wang, X., Ilghari, D., and Li, X. A novel solid-phase site-specific PEGylation enhances the in vitro and in vivo biostabilty of recombinant human keratinocyte growth factor 1. *PLoS One* 2012 May; **7**(5): e36423.

23. Zhang, Y., Velasco, O., Zhang, X., Ting, K., Soo, C., and Wu, B.M. Bioactivity and circulation time of PEGylated NELL-1 in mice and the potential for osteoporosis therapy. *Biomaterials* 2014 Aug; 35(24): 6614-6621.

24. Kuroda S, Oyasu M, Kawakami M*, et al.* Biochemical characterization and expression analysis of neural thrombospondin-1-like proteins NELL1 and NELL2. *Biochemical and biophysical research communications* 1999 Nov; **265**(1)**:** 79-86.

25. Campbell ID, Baron M. The Structure And Function Of Protein Modules. *Philos T Roy Soc B* 1991 May 29; **332**(1263)**:** 165-170.

26. Abreu JG, Coffinier C, Larrain J, Oelgeschlager M, De Robertis EM. Chordin-like CR domains and the regulation of evolutionarily conserved extracellular signaling systems. *Gene* 2002 Apr 3; **287**(1-2)**:** 39-47.

27. Spiegel I, Salomon D, Erne B, Schaeren-Wiemers N, Peles E. Caspr3 and caspr4, two novel members of the caspr family are expressed in the nervous system and interact with PDZ domains. *Molecular and cellular neurosciences* 2002 Jun; **20**(2)**:** 283-297.

28. Karayannis T, Au E, Patel JC*, et al.* Cntnap4 differentially contributes to GABAergic and dopaminergic synaptic transmission. *Nature* 2014 Jul 10; **511**(7508)**:** 236-240.

29. Yin FT, Futagawa T, Li D*, et al.* Caspr4 Interaction with LNX2 Modulates the Proliferation and Neuronal Differentiation of Mouse Neural Progenitor Cells. *Stem cells and development* 2015 Mar 1; **24**(5)**:** 640-652.

30. Gordon J, Amini S, White MK. General overview of neuronal cell culture. *Methods in molecular biology* 2013; **1078:** 1-8.

31. Trapnell C, Roberts A, Goff L*, et al.* Differential gene and transcript expression analysis of RNA-seq experiments with TopHat and Cufflinks. *Nat Protoc* 2012 Mar; **7**(3)**:** 562-578.

32. Zou X, Shen J, Chen F*, et al.* NELL-1 binds to APR3 affecting human osteoblast proliferation and differentiation. *FEBS letters* 2011 Aug 4; **585**(15)**:** 2410-2418.

33. Zhang X, Ting K, Bessette CM*, et al.* Nell-1, a key functional mediator of Runx2, partially rescues calvarial defects in Runx2(+/-) mice. *Journal of bone and mineral research : the official journal of the American Society for Bone and Mineral Research* 2011 Apr; **26**(4)**:** 777-791.

34. Kalueff AV, Aldridge JW, LaPorte JL, Murphy DL, Tuohimaa P. Analyzing grooming microstructure in neurobehavioral experiments. *Nat Protoc* 2007; **2**: 2538-2544.

35. Deacon RM. Digging and marble burying in mice: simple methods for in vivo identification of biological impacts. *Nat Protoc* 2006; **1**: 122-124.

36. Terzian AL, Drago F, Wotjak CT, Micale V. The Dopamine and Cannabinoid Interaction in the Modulation of Emotions and Cognition: Assessing the Role of Cannabinoid CB1 Receptor in Neurons Expressing Dopamine D1 Receptors. *Front Behav Neurosci* 2011 Aug; **5**, 49.

37. Arnsdorf EJ, Jones LM, Cater DR, Jacobs CR. Multipotent Characteristics of Periosteal Cells and Fibroblasts. In: Arnsdorf EJ (ed). *Guiding Osteogenic Lineage Commitment: The Role of Mesenchymal Stem Cell Biology and the Mechanical Microenvironment*. ProQuesst LLC2008.

38. Yazid MD, Ariffin SHZ, Senafi S, Razak MA, Wahab RMA. Determination of the differentiation capacities of murines' primary mononucleated cells and MC3T3-E1 cells. *Cancer Cell Int* 2010 Oct 28; **10**.

39. Mohseny AB, Machado I, Cai YP*, et al.* Functional characterization of osteosarcoma cell lines provides representative models to study the human disease. *Laboratory Investigation* 2011 Aug; **91**(8)**:** 1195-1205.

40. Tsai SW, Liou HM, Lin CJ*, et al.* MG63 Osteoblast-Like Cells Exhibit Different Behavior when Grown on Electrospun Collagen Matrix versus Electrospun Gelatin Matrix. *Plos One* 2012 Feb 2; **7**(2).

41. Thompson L, Wang SS, Tawfik O*, et al.* Effect of 25-hydroxyvitamin D3 and 1 alpha,25 dihydroxyvitamin D-3 on differentiation and apoptosis of human osteosarcoma cell lines. *J Orthop Res* 2012 May; **30**(5)**:** 831-844.

42. Taylor SM, Jones PA. Multiple New Phenotypes Induced In 10t1/2-Cells And 3t3-Cells Treated with 5-Azacytidine. *Cell* 1979; **17**(4)**:** 771-779.

43. Rohilla M, Bal A, Singh G, Joshil K. Phenotypic and Functional Characterization of Ductal Carcinoma In Situ-Associated Myoepithelial Cells. *Clin Breast Cancer* 2015 Oct; **15**(5)**:** 335-342.

44. Yao Y, Wang Y. ATDC5: an excellent in vitro model cell line for skeletal development. *Journal of cellular biochemistry* 2013 Jun; **114**(6)**:** 1223-1229.

45. Bokui N, Otani T, Igarashi K*, et al.* Involvement of MAPK signaling molecules and Runx2 in the NELL1-induced osteoblastic differentiation. *FEBS letters* 2008 Jan 23; **582**(2)**:** 365-371.

46. Chen F, Walder B, James AW*, et al.* NELL-1-dependent mineralisation of Saos-2 human osteosarcoma cells is mediated via c-Jun N-terminal kinase pathway activation. *International orthopaedics* 2012 Oct; **36**(10)**:** 2181-2187.

47. Zhang X, Cowan CM, Jiang X*, et al.* Nell-1 induces acrania-like cranioskeletal deformities during mouse embryonic development. *Laboratory investigation; a journal of technical methods and pathology* 2006 Jul; **86**(7)**:** 633-644.

48. Matsumoto A, Hatta T, Moriyama K, Otani H. Sequential observations of exencephaly and subsequent morphological changes by mouse exo utero development system: analysis of

the mechanism of transformation from exencephaly to anencephaly. *Anat Embryol* 2002 Jan; **205**(1)**:** 7-18.

49. Chen W, Zhang X, Siu RK*, et al.* Nfatc2 is a primary response gene of Nell-1 regulating chondrogenesis in ATDC5 cells. *Journal of bone and mineral research : the official journal of the American Society for Bone and Mineral Research* 2011 Jun; **26**(6)**:** 1230-1241.

50. Ding X, Chen Y, Han L, Qiu W, Gu X, Zhang H. Apoptosis related protein 3 is a lysosomal membrane protein. *Biochemical and biophysical research communications* 2015 May 15; **460**(4)**:** 915-922.

51. Hasebe A, Nakamura Y, Tashima H*, et al.* The C-terminal region of NELL1 mediates osteoblastic cell adhesion through integrin alpha3beta1. *FEBS letters* 2012 Jul 30; **586**(16)**:** 2500-2506.

52. Shen J, James AW, Chung J*, et al.* NELL-1 promotes cell adhesion and differentiation via Integrinbeta1. *Journal of cellular biochemistry* 2012 Dec; **113**(12)**:** 3620-3628.

53. Goessler UR, Bugert P, Bieback K*, et al.* Integrin expression in stem cells from bone marrow and adipose tissue during chondrogenic differentiation. *International journal of molecular medicine* 2008 Mar; **21**(3)**:** 271-279.

54. Loeser RF. Integrins and chondrocyte-matrix interactions in articular cartilage. *Matrix Biol* 2014 Oct; **39:** 11-16.

55. Masi L. Crosstalk between the brain and bone. *Clinical cases in mineral and bone metabolism: the official journal of the Italian Society of Osteoporosis, Mineral Metabolism, and Skeletal Diseases* 2012 Jan; **9**(1)**:** 13-16.

56. Lieblein-Boff JC, Johnson EJ, Kennedy AD, Lai CS, Kuchan MJ. Exploratory Metabolomic Analyses Reveal Compounds Correlated with Lutein Concentration in Frontal Cortex, Hippocampus, and Occipital Cortex of Human Infant Brain. *Plos One* 2015; **10**(8)**:** e0136904.

57. Zheng QP, Cai XH, Tan MH*, et al.* Precise gene deletion and replacement using the CRISPR/Cas9 system in human cells. *Biotechniques* 2017 Jan; **62**(1).

58. Chen X, Xie C, Sun L, Ding J, Cai H. Longitudinal Metabolomics Profiling of Parkinson's Disease-Related alpha-Synuclein A53T Transgenic Mice. *Plos One* 2015; **10**(8)**:** e0136612.

59. Nakamura R, Nakamoto C, Obama H, Durward E, Nakamoto M. Structure-function analysis of Nel, a thrombospondin-1-like glycoprotein involved in neural development and functions. *The Journal of biological chemistry* 2012 Jan 27; **287**(5)**:** 3282-3291.

60. Ran FA, Hsu PD, Lin CY*, et al.* Double nicking by RNA-guided CRISPR Cas9 for enhanced genome editing specificity. *Cell* 2013 Sep 12; **154**(6)**:** 1380-1389.

61. Altmaier E, Emeny RT, Krumsiek J*, et al.* Metabolomic profiles in individuals with negative affectivity and social inhibition: a population-based study of Type D personality. *Psychoneuroendocrinology* 2013 Aug; **38**(8)**:** 1299-1309.

62. Hinard V, Mikhail C, Pradervand S*, et al.* Key Electrophysiological, Molecular, and Metabolic Signatures of Sleep and Wakefulness Revealed in Primary Cortical Cultures. *J Neurosci* 2012 Sep 5; **32**(36)**:** 12506-12517.

63. Bauer DE, Canver MC, Orkin SH. Generation of genomic deletions in mammalian cell lines via CRISPR/Cas9. *Journal of visualized experiments: JoVE* 2015 Jan 03; (95)**:** e52118.

64. Zheng QP, Cai XH, Tan MH*, et al.* Precise gene deletion and replacement using the CRISPR/Cas9 system in human cells. *Biotechniques* 2014 Sep; **57**(3)**:** 115-124.